

Myofibroblasts are the main effector cells in the fibrotic liver. In both experimental and clinical liver fibrosis cases, myofibroblasts appear and produce ECM at the site of the hepatic injury. The activation of ordinarily quiescent hepatic stellate cells (HSCs) into myofibroblasts is considered a major pathway of hepatic fibrogenesis associated with liver injury and has thus dominated the focus of studies on liver fibrosis [5]. The activated HSCs or their resulting myofibroblasts were the first major cell type in the liver to be identified as prominent in producing ECM in the injured liver [6]. Currently, at least three sources of myofibroblasts in liver fibrosis have been proposed. The hepatic resident mesenchymal cells [7], consisting of the quiescent HSCs and the portal fibroblasts, can differentiate into myofibroblasts. Then, bone-marrow derived cells, consisting of fibrocytes and mesenchymal stem cells in the peripheral blood, can be recruited to the injured liver to differentiate into myofibroblasts. Recent studies have demonstrated that bone-marrow derived cells make only a small contribution to the myofibroblast population in experimental liver fibrosis. Instead, fibrocytes may play a crucial role in the initiation of immune response during the earliest phases of tissue injury [8•]. Finally, hepatic progenitor cells, hepatocytes, cholangiocytes, and hepatic sinusoidal endothelial cells have been proposed to differentiate into myofibroblasts through epithelial or endothelial mesenchymal transition (EMT). Although primary hepatocytes can undergo EMT *in vitro*, it is extremely hard to detect hepatic myofibroblasts originating from epithelial or endothelial cells through EMT *in vivo* [9]. Thus, the main sources of hepatic myofibroblasts in liver fibrosis are the hepatic resident mesenchymal cells, consisting of the HSCs and portal fibroblasts. The most widely used and accessible marker of myofibroblasts are the *de novo* expression of α -smooth muscle actin (α -SMA). However, no reliable markers have yet been identified for distinguishing HSCs from portal fibroblasts after myofibroblastic differentiation. The contribution of portal fibroblasts to hepatic fibrosis is not well understood mainly because of the difficulties in distinguishing and isolating them.

Development of liver fibrosis and cirrhosis is associated with deposition of ECM, in which Collagen Type I is the most abundant [10]. Transgenic Collagen- α 1(I)-GFP mice have been generated a decade ago. In these mice expression of GFP is driven by Collagen- α 1(I) promoter, and therefore, expression of GFP is observed in cells that upregulate Collagen Type I. Our current review will summarize the recent results obtained from transgenic reporter mice and novel flow cytometry protocols developed to distinguish HSC- and portal fibroblast-derived myofibroblasts and quantify their relative contributions to hepatic fibrosis.

Fibrotic Cascade in the Liver

Once hepatic epithelial cells (hepatocytes and/or cholangiocytes) are damaged by any cause, inflammatory mediators are released to initiate a series of responses to liver injury. Inflammatory cells recruited to the site of injury phagocytose necrotic or apoptotic cells and amplify the inflammatory response by releasing pro-inflammatory cytokines, such as tumor necrosis factor- α (TNF- α), interleukin-6 (IL-6), and interleukin-1 beta (IL-1 β), and by recruiting T cells [11]. The hepatic mesenchymal precursor cells of myofibroblasts are activated and differentiated by growth factors and cytokines including transforming growth factor-beta (TGF- β), platelet-derived growth factor (PDGF), and interleukin-13 (IL-13). TGF- β drives myofibroblast activation and ECM synthesis. PDGF stimulates HSC proliferation through its positive feedback mechanism involved in the autocrine and paracrine effect. IL-13 has been also implicated in stimulation of TGF- β synthesis in cells [12].

Immune cells play a pivotal role in the development of hepatic fibrosis. In experimentally induced fibrosis, the balance between Th1 and Th2 cells is important for the fibrotic response. For example, C57BL/6 mice (in which a Th1 cell response predominates) have a lower fibrotic reaction than BALB/c mice (in which a Th2 cell response predominates) [13]. Recently, increasing evidence has suggested an emerging novel role of T cell subsets, including Th17, Treg, and $\delta\gamma$ T cells, in the fibrotic process [14]. However, further studies are needed to fully elucidate their functions.

Hepatic fibrosis is a dynamic process and can be considered a part of the healing response to liver injury. The ECM is not stable, but is constantly synthesized and degraded by proteolytic enzymes such as the matrix metalloproteinases (MMP) or collagenases. The reversibility of mild to moderate hepatic fibrosis is now a reality in patients whose etiology has been successfully treated. In clinical practice, studies of antiviral treatments for hepatitis C have showed that fibrosis is reversible after a sustained virologic response [15]. However, there is no unequivocal evidence for a complete reversal of severe cirrhosis with regenerative nodules and dense fibrotic septa. Current clinical studies based on liver biopsies have showed that the matrix enzyme lysyl oxidase-like-2 (LOXL2) increased in the fibrotic liver and was limited in the healthy liver. LOXL2 catalyzes the first step in the formation of crosslinks in fibrillar collagen. The extensiveness of the crosslinks observed in severe fibrosis and cirrhosis prevent their degradation by collagenases [16].

Hepatic Myofibroblasts

Hepatic myofibroblasts, characterized by expression of α -SMA and production of ECM, are mainly found in chronically injured livers, irrespective of the etiology, and are morphologically defined as large and spindle-shaped cells with cytoplasmic stress fibers running parallel to the long axis. Myofibroblasts are characterized by several common features based on their ultrastructural analysis, including a prominent rough endoplasmic reticulum, a Golgi apparatus producing collagen, peripheral myofilaments, well-developed cell-to-stroma attachment sites (fibronexus), and gap junctions [17, 18]. The process of myofibroblast differentiation leads to a highly proliferative, migratory, and contractile phenotype. The persisting inflammation is believed to drive and sustain fibrogenesis. Myofibroblasts can release a number of pro-inflammatory molecules and directly contribute to this continuous inflammation [10, 19, 20]. In both experimental and clinical liver fibrosis, there is a close correlation between the regression of liver fibrosis and the disappearance of myofibroblasts. Previous studies have demonstrated that some myofibroblasts undergo cell death by apoptosis, while other myofibroblasts are restored to their quiescent-like state [21, 22]. This phenomenon has been identified recently, but has a great potential for anti-fibrotic therapy. However, the mechanism underlying “inactivation” of HSC/myofibroblasts in response to toxic liver injury remains unknown. Future investigations are required to determine why a half of HSC/myofibroblasts apoptose during regression of liver fibrosis, while the other half of myofibroblasts survives and undergoes inactivation. Identification of the mechanism of HSC/myofibroblast inactivation, may provide new targets for anti-fibrotic therapy.

Two Experimental Models for the Study of Hepatic Fibrosis

Mouse models have been used for several decades to study fibrogenesis. The two most common methods for modeling experimental liver fibrosis in mice are the administration of carbon tetrachloride (CCl_4) and bile duct ligation (BDL). Each model displays specific characteristics in the evolution of fibrosis.

Administration of CCl_4 leads to centrilobular necrosis, and eventually leads to liver fibrosis and cirrhosis. CCl_4 causes damage of hepatocytes, in which highly reactive free radical metabolites are formed by the mixed function oxidase system, including a CYP2E1-mediated reaction [23]. HSCs are activated following CCl_4 challenges. In this model, fibrosis first develops in pericentral areas and secondarily between central and portal areas, which is called “bridging fibrosis.”

The hepatic injury induced by BDL in mice is similar to the condition of human secondary biliary cirrhosis; it is characterized by cholestasis, hepatic inflammation, neutrophil infiltration in the portal tracts, proliferation of cholangiocytes, and portal tract fibrosis. In BDL mice, serum bile acid levels increase by dozens of fold. Bile acids are pro-oxidants directly causing tissue damage mediated by reactive oxygen species (ROS), or indirectly through activation of Kupffer cells to release ROS [24]. The overflow of bile acid stimulates the proliferation of cholangiocytes, resulting in a ductular reaction accompanied by portal inflammation and fibrosis [25]. Previous studies have showed the importance of portal fibroblasts as contributors to fibrosis in the BDL model [26].

Hepatic Stellate Cells (HSCs)

HSCs are intralobular connective tissue cells representing less than ten percent of the total number of liver cells. Under physiological conditions, HSCs reside in the space of Disse and serve as a major storage of Vitamin A in the mammalian body. HSCs also participate in the homeostasis of the intrahepatic ECM protein turnover by secreting the sufficient amount of ECM molecules required for tissue repair and by releasing MMP and their inhibitors. By virtue of the contractility of their long cytoplasmic processes encircling the sinusoid, HSCs presumably contribute to the regulation of hepatic microcirculation through the sinusoidal capillaries [27].

The liver is the main storage organ for dietary Vitamin A. Vitamin A includes numerous retinoid forms such as retinyl esters, retinol, retinal, retinoic acid, and several provitamin A carotenoids. Retinoids are transported in the form of retinyl esters. Dietary retinoids are absorbed in the small intestine, where they are packaged into chylomicrons for transportation to the lymphatic circulation system. The retinoid-containing chylomicrons are taken up by hepatocytes, wherein retinoids are hydrolyzed to retinol, and bound retinol-binding protein (RBP), to transfer to the HSCs for storage. HSCs are the central cellular site for retinoid storage in healthy animals, accounting for as much as 50–60 % of the total retinoid present in the entire body. Retinoids are stored in the form of retinyl esters in the lipid droplets, which are characteristic of HSCs [28]. In response to liver injury, quiescent HSCs activate and release some of the Vitamin A droplets. Upon activation, HSCs change their morphology, migrate to the site of injury, and upregulate mesenchymal markers such as α -SMA, collagen α 1(I), and fibronectin. HSCs differentiate into myofibroblasts in the injured liver and produce ECM [29].

Portal fibroblasts

Portal fibroblasts are resident fibroblasts with a spindle shape which are present in very small numbers in the mesenchyme surrounding the bile ducts. Under normal conditions, they participate in physiological ECM turnover. Portal fibroblasts almost certainly give rise to myofibroblasts during the development of cholestatic liver injury (but not toxic liver injury, [30]). In response to hepatic injury induced by BDL in mice, portal fibroblasts proliferate and are activate to produce ECM at the periphery of the bile ducts [31]. Portal fibroblasts can be distinguished from HSCs due to the lack of oil droplets, including Vitamin A. In addition, they express elastin and Thy-1; elastin, fibulin 2, gremlin 1, and mesothelin (a novel marker) have also been identified as markers of portal fibroblasts [32, 33]. However, during the development of hepatic injury, HSCs slightly express elastin [34]. Thy1 is a T cell marker, which is particularly abundant on the surface of thymocytes and peripheral T cells. Therefore, the question is, what are the specific markers for portal fibroblasts, and how portal fibroblasts can be distinguished from other myofibroblasts in fibrotic liver. In chronic cholestatic disorders, the fibrotic tissue is initially located around portal tracts. Histological findings from fibrotic livers suggested that portal fibroblasts contribute to the overall fibroblasts observed in cholestatic liver injury. However, their role in liver fibrosis is still unclear because of the lack of markers that can definitively determine the presence of portal fibroblasts from the pool of hepatic myofibroblasts. This problem is further complicated by a recent report by Asahina et al., suggesting that portal fibroblasts and HSCs may originate from a common progenitor during the embryonic development [7].

Strategies to Detect Hepatic Myofibroblasts

In recent years, manipulation of mouse genetics has been remarkably progressed and provided tools that have greatly facilitated the studies designed to dissect many biological processes in mammalian body, including liver fibrosis. Thus, development of collagen- $\alpha 1(I)$ -GFP mice became one of the useful tools to study liver fibrosis [9, 17, 21, 35]. Our group has also utilized the collagen- $\alpha 1(I)$ -GFP transgenic mouse in which green fluorescent protein (GFP) is upregulated in hepatic myofibroblasts in response to fibrogenic liver injury [36]. These mice can undergo chronic liver injury with repeated CCl₄ injections or BDL to induce liver fibrosis, after which their collagen-producing cells express GFP, which is easily identified by its GFP fluorescence. The expression of collagen- $\alpha 1(I)$ -driven GFP

in these mice closely correlates with the expression of α -SMA, a general marker for myofibroblasts. The GFP-expressing cells have been considered myofibroblasts [35]. Our strategy to detect hepatic myofibroblasts was based on the investigation of GFP-expressing cells in nonparenchymal fractions of CCl₄-treated or BDL collagen- $\alpha 1(I)$ -GFP mice.

The study of the cell fate mapping of HSCs had demonstrated that although there is a decrease in the amount of Vitamin A upon HSC activation, the Vitamin A-specific autofluorescence excited with UV can be still detected in all HSCs by flow cytometry [35, 37]. Whereas the GFP is expressed in all myofibroblasts, the presence of droplets containing of Vitamin A is solely and exclusively attributed to HSC-derived myofibroblasts [35, 37, 38]. To distinguish HSCs from hepatic myofibroblasts of other origins, the flow cytometry has been reported to be a method of choice to distinguish and quantify the contribution of HSCs and portal fibroblasts to liver fibrosis induced by either CCl₄ treatment or BDL. The suggested method used GFP to identify all myofibroblasts. Next, the presence of Vitamin A was used to identify myofibroblasts originated from HSCs, while all other GFP + Vitamin A- myofibroblasts were attributed to myofibroblasts of all other origins. Surprisingly, this GFP + Vitamin A- fraction was composed mostly by Thy1 and TE-1 (elastin) positive cells, while CD45 + Collagen- $\alpha 1(I)$ -GFP + fibrocytes [39] constituted only 4 % of total GFP + fraction. Taken together, the flow cytometry-based quantification analysis of hepatic myofibroblasts activated in fibrotic liver in response to different types of liver injury (toxic and cholestatic) has demonstrated that HSCs are the major source of myofibroblasts in CCl₄-induced liver fibrosis. However, portal fibroblasts are the major source of myofibroblasts at the onset of BDL-induced liver injury, within a week of BDL. The relative contribution of portal fibroblasts decreases upon chronic cholestatic injury, as HSCs become progressively activated and contribute to the myofibroblast population. Remarkably, the phenotype of BDL-activated HSCs has more similarities with BDL-activated portal fibroblasts rather than with CCl₄-activated HSCs, suggesting that portal fibroblasts might affect (or even regulate) activation of HSCs in BDL-injured liver.

This observation was supported by the gene expression array. Both of these cellular populations were isolated from mouse liver by flow cytometry and the gene expression profile was determined for GFP + Vitamin A + and GFP + Vitamin A- populations from CCl₄- and BDL-injured mice. Gene expression profiling and complimentary immunohistochemistry revealed that myofibroblasts

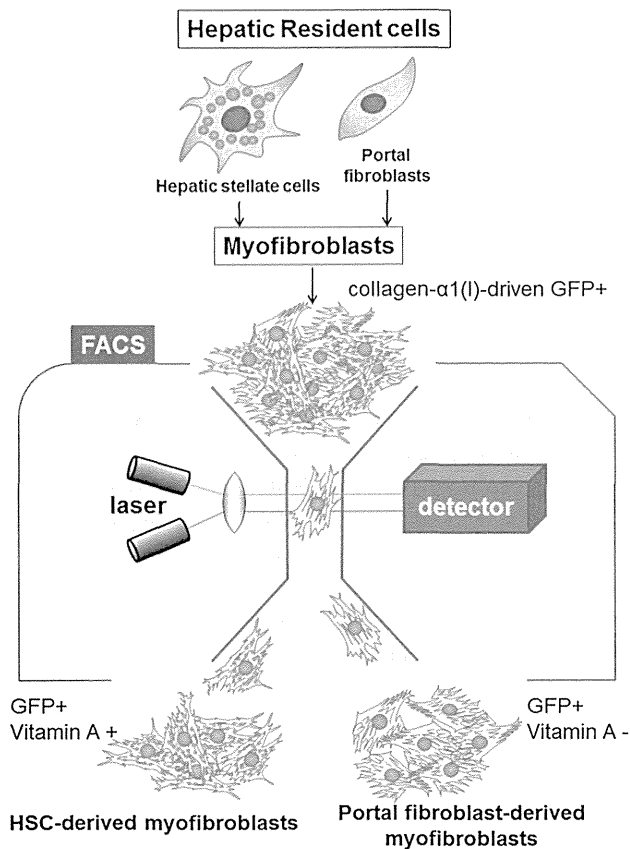


Fig. 1 Strategy to analysis myofibroblasts by flow cytometry: Myofibroblasts expressing collagen- $\alpha 1(I)$ -driven GFP+ are identified in nonparenchymal fraction by argon laser at 488 nm wavelength and further fractionated to Vitamin A+ and Vitamin A- cells by UV laser. HSC-derived myofibroblasts are sort-purified as the GFP+ and Vitamin A+ fraction. Portal fibroblast-derived myofibroblasts are sort-purified as the GFP+ and Vitamin A- fraction

derived from HSCs are positive for desmin, and myofibroblasts derived from portal fibroblasts express Thyl, elastin, and mesothelin [35]. Mesothelin is a membrane glycoprotein that is expressed in normal mesothelial cells; however, its function is not clear. In our study, mesothelin was highly expressed in myofibroblasts derived from portal fibroblasts, such that mesothelin may serve as a novel marker of portal fibroblasts. Despite this finding, the function of mesothelin in mice or humans is not yet clear. In addition, recent studies have suggested that liver capsule (which may also express mesothelial markers) can contribute to hepatic myofibroblasts in response to fibrogenic liver injury [7, 40]. At this time, it remains unclear if the mesothelin+ myofibroblasts represent heterogeneous population of hepatic mesenchymal cells that emerge in the damaged liver in response to chronic injury, or is comprised by the same cell type at different stages of activation. Taken together, there might be two major sources of

hepatic myofibroblasts in fibrotic liver [39•]. These populations of myofibroblasts may behave similar to each other (Fig. 1), but they exhibit unique properties, and can be distinguished from each other based on their gene expression profile. Therefore, we emphasize that the composition of myofibroblasts varies depending on the etiology of the hepatic injury, and the origin of myofibroblasts may determine the personalized anti-fibrotic therapy of patients with liver fibrosis of different etiologies [35••, 41].

Conclusions

Myofibroblasts are the source of the fibrous scar tissue in liver fibrosis. Hepatic myofibroblasts are transdifferentiated from two main cell populations in response to hepatic injury. The major origins of hepatic myofibroblasts are HSCs and portal fibroblasts. Fibrocytes also contribute to liver fibrosis but their function is not well characterized. Liver fibrosis caused by hepatotoxic injury is attributed to the activated HSCs. However, portal fibroblasts are implicated in liver fibrosis induced by cholestatic liver injury. The contribution of portal fibroblasts to liver fibrosis has not been well characterized because of the difficulties in cell sorting-purification and the lack of identifiable and specific markers for portal fibroblasts. Our novel flow cytometry method makes it possible to distinguish HSC- and portal fibroblast-derived myofibroblasts from the nonparenchymal cell fraction of the fibrotic liver in mice. It is also able to identify a novel specific marker, mesothelin, which is specific to portal fibroblasts. A detailed investigation of myofibroblasts, particularly using new methods such as ours, will provide insight into the mechanisms underlying liver fibrosis, and may lead to the development of more effective therapy.

Open Access This article is distributed under the terms of the Creative Commons Attribution License which permits any use, distribution, and reproduction in any medium, provided the original author(s) and the source are credited.

Compliance with Ethics Guidelines

Conflict of interest Keiko Iwaisako declares a Grant from The Ministry of Education, Culture, Sports, Science and Technology of Japan (No. 26461909), a Grant from Kobayashi Foundation for Cancer Research and a Grant from The Ministry of Health, Labour, and Welfare which are unrelated to this article. Kojiro Taura declares a Grant from The Ministry of Education, Culture, Sports, Science and Technology of Japan (No. 25670575) which is unrelated to this article. Masataka Asagiri declares a Grant from The Ministry of Education, Culture, Sports, Science and Technology of Japan (No. 24659822), a Grant from The Ministry of Education, Culture, Sports, Science and Technology of Japan (No. 24689056) and a Grant from The Ministry of Health, Labour, and Welfare of Japan which are

unrelated to this article. Yukinori Koyama and Kenji Takemoto declare no conflicts of interest.

Human and Animal Rights and Informed Consent This article does not contain any studies with human or animal subjects performed by any of the authors.

References

Papers of particular interest, published recently, have been highlighted as:

- Of importance
- Of major importance

1. Friedman SL (2008) Mechanisms of hepatic fibrogenesis. *Gastroenterology* 134:1655–1669. doi:10.1053/j.gastro.2008.03.003
2. Zhang DY, Friedman SL (2012) Fibrosis-dependent mechanisms of hepatocarcinogenesis. *Hepatology* 56:769–775. doi:10.1002/hep.25670
3. Murray KF, Carithers RL Jr, AASLD (2005) AASLD practice guidelines: evaluation of the patient for liver transplantation. *Hepatology* 41:1407–1432
4. Pellicoro A et al (2014) Liver fibrosis and repair: immune regulation of wound healing in a solid organ. *Nat Rev Immunol* 14:181–194. doi:10.1038/nri3623
5. Friedman SL (1999) The virtuosity of hepatic stellate cells. *Gastroenterology* 117:1244–1246
6. Lee UE, Friedman SL (2011) Mechanisms of hepatic fibrogenesis. *Best Pract Res Clin Gastroenterol* 25:195–206. doi:10.1016/j.bpg.2011.02.005
7. Lua I et al (2014) Mesodermal mesenchymal cells give rise to myofibroblasts, but not epithelial cells, in mouse liver injury. *Hepatology* 60:311–322. doi:10.1002/hep.27035
8. • Brenner DA et al (2012) Origin of myofibroblasts in liver fibrosis. *Fibrogenesis Tissue Repair* 6:S17. *The authors summarize that the origin of myofibroblasts are different for different types of chronic liver diseases*
9. Taura K et al (2010) Hepatocytes do not undergo epithelial-mesenchymal transition in liver fibrosis in mice. *Hepatology* 51:1027–1036. doi:10.1002/hep.23368
10. Bataller R, Brenner DA (2005) Liver fibrosis. *J Clin Invest* 115:109–118
11. Jenne CN, Kubes P (2013) Immune surveillance by the liver. *Nat Immunol* 14:996–1006. doi:10.1038/ni.2691
12. Liu Y et al (2012) IL-13 signaling in liver fibrogenesis. *Front Immunol* 3:116. doi:10.3389/fimmu.2012.00116
13. Shi Z, Wakil AE, Rockey DC (1997) Strain-specific differences in mouse hepatic wound healing are mediated by divergent T helper cytokine responses. *Proc Natl Acad Sci USA* 94:10663–10668
14. Li J et al (2012) Significance of the balance between regulatory T (Treg) and T helper 17 (Th17) cells during hepatitis B virus related liver fibrosis. *PLoS One* 7:e39307. doi:10.1371/journal.pone.0039307
15. Iredale JP, Thompson A, Henderson NC (2013) Extracellular matrix degradation in liver fibrosis: biochemistry and regulation. *Biochim Biophys Acta* 1832:876–883. doi:10.1016/j.bbadis.2012.11.002
16. Barry-Hamilton V et al (2010) Allosteric inhibition of lysyl oxidase-like-2 impedes the development of a pathologic microenvironment. *Nat Med* 16:1009–1017. doi:10.1038/nm.2208
17. Eyden B (2008) The myofibroblast: phenotypic characterization as a prerequisite to understanding its functions in translational medicine. *J Cell Mol Med* 12:22–37. doi:10.1111/j.1582-4934.2007.00213.x
18. Schürch W et al (1998) The myofibroblast: a quarter century after its discovery. *Am J Surg Pathol* 22:141–147
19. Scholten D et al (2011) Migration of fibrocytes in fibrogenic liver injury. *Am J Pathol* 179:189–198. doi:10.1016/j.ajpath.2011.03.049
20. Parola M, Marra F, Pinzani M (2008) Myofibroblast-like cells in liver fibrogenesis: emerging concepts in a rapidly moving scenario. *Mol Asp Med* 29:58–66
21. • Kisseleva T et al (2012) Myofibroblasts revert to an inactive phenotype during regression of liver fibrosis. *Proc Natl Acad Sci USA* 109:9448–9453. doi: 10.1073/pnas.1201840109. *This study by using genetic labeling of aHSCs/myofibroblasts demonstrates that some aHSCs escape cell death and revert to an inactivated phenotype*
22. Troeger JS et al (2012) Deactivation of hepatic stellate cells during liver fibrosis resolution in mice. *Gastroenterology* 143(1073–83):e22. doi:10.1053/j.gastro.2012.06.036
23. Shi J et al (1998) Evidence of hepatocyte apoptosis in rat liver after the administration of carbon tetrachloride. *Am J Pathol* 153:515–525
24. Ljubuncic P, Tanne Z, Bomzon A (2000) Evidence of a systemic phenomenon for oxidative stress in cholestatic liver disease. *Gut* 47:710–716
25. Desmet VJ (2011) Ductal plates in hepatic ductular reactions. Hypothesis and implications. I. Types of ductular reaction reconsidered. *Virchows Arch* 458:251–259. doi:10.1007/s00428-011-1048-3
26. Popov Y et al (2010) Macrophage-mediated phagocytosis of apoptotic cholangiocytes contributes to reversal of experimental biliary fibrosis. *Am J Physiol Gastrointest Liver Physiol* 298:G323–G334. doi:10.1152/ajpgi.00394.2009
27. Senoo H et al (2010) Hepatic stellate cell (vitamin A-storing cell) and its relative—past, present and future. *Cell Biol Int* 34:1247–1272. doi:10.1042/CBI20100321
28. Blaner WS et al (2009) Hepatic stellate cell lipid droplets: a specialized lipid droplet for retinoid storage. *Biochim Biophys Acta* 1791:467–473. doi:10.1016/j.bbali.2008.11.001
29. Shirakami Y et al (2012) Hepatic metabolism of retinoids and disease associations. *Biochim Biophys Acta* 1821:124–136. doi:10.1016/j.bbali.2011.06.023
30. Wells RG (2014) The portal fibroblast: not just a poor man's stellate cell. *Gastroenterology* 147:41–47. doi:10.1053/j.gastro.2014.05.001
31. Wells RG, Kruglov E, Dranoff JA (2004) Autocrine release of TGF-beta by portal fibroblasts regulates cell growth. *FEBS Lett* 559:107–110
32. Li Z et al (2007) Transforming growth factor-and substrate stiffness regulate portal fibroblast activation in culture. *Hepatology* 46:1246–1256
33. Motoyama H et al (2014) Cytoglobin is expressed in hepatic stellate cells, but not in myofibroblasts, in normal and fibrotic human liver. *Lab Invest* 94:192–207. doi:10.1038/labinvest.2013.135
34. Perepeyuk M et al (2013) Hepatic stellate cells and portal fibroblasts are the major cellular sources of collagens and lysyl oxidases in normal liver and early after injury. *Am J Physiol Gastrointest Liver Physiol* 304:G605–G614. doi:10.1152/ajpgi.00222.2012
35. •• Iwasako K et al (2014) Origin of myofibroblasts in the fibrotic liver in mice. *Proc Natl Acad Sci USA* 29. pii: 201400062. [Epub ahead of print] *This study demonstrates that the novel flow cytometry-based method enables identification of hepatic myofibroblasts and isolation of distinct subsets of myofibroblasts*
36. Yata Y et al (2003) DNase I-hypersensitive sites enhance alpha1(I) collagen gene expression in hepatic stellate cells. *Hepatology* 37:267–276

37. Mederacke I et al (2013) Fate tracing reveals hepatic stellate cells as dominant contributors to liver fibrosis independent of its aetiology. *Nat Commun* 4:2823. doi:10.1038/ncomms3823
38. Kisseleva T, Brenner DA (2013) Inactivation of myofibroblasts during regression of liver fibrosis. *Cell Cycle* 12:381–382. doi:10.4161/cc.23549
39. • Kisseleva T, Brenner DA (2012) The phenotypic fate and functional role for bone marrow-derived stem cells in liver fibrosis. *J Hepatol* 56:965–972. doi: 10.1016/j.jhep.2011.09.021.
40. Li Y et al (2013) Mesothelial cells give rise to hepatic stellate cells and myofibroblasts via mesothelial-mesenchymal transition in liver injury. *Proc Natl Acad Sci USA* 110:2324–2329. doi:10.1073/pnas.1214136110
41. Kisseleva T, Brenner DA (2011) Anti-fibrogenic strategies and the regression of fibrosis. *Best Pract Res Clin Gastroenterol* 25:305–317. doi:10.1016/j.bpg.2011.02.011

The authors summarize that bone marrow derived cells play an important role in pathogenesis and resolution of liver fibrosis

Evaluation of hepatocellular carcinoma development in patients with chronic hepatitis C by EOB-MRI

Shunsuke Nojiri, Kei Fujiwara, Noboru Shinkai, Mio Endo, Takashi Joh

Shunsuke Nojiri, Kei Fujiwara, Noboru Shinkai, Mio Endo, Takashi Joh, Department of Gastroenterology and Metabolism, Nagoya City University Graduate School of Medical Sciences, Nagoya, Aichi 467-8601, Japan

Author contributions: Nojiri S is the author; Fujiwara K, Shinkai N, Endo M and Joh T contributed to collecting data.

Correspondence to: Shunsuke Nojiri, MD, PhD, Department of Gastroenterology and Metabolism, Nagoya City University Graduate School of Medical Sciences, Kawasumi 1, Mizuho-cho, Mizuho-ku, Nagoya, Aichi 467-8601,

Japan. snojiri@med.nagoya-cu.ac.jp

Telephone: +81-52-8538211 Fax: +81-52-8520952

Received: July 9, 2014 Revised: October 22, 2014

Accepted: November 17, 2014

Published online: December 27, 2014

and LI < 1.46 were identified as independent factors, but on multivariate analysis, LI < 1.46: risk ratio 6.05 (1.34-27.3, $P = 0.019$) and AFP ≥ 10 : risk ratio 3.1 (1.03-9.35, $P = 0.045$) were identified as independent risk factors. LI and Fib-4 index have higher area under the receiver operating characteristic curves than other representative fibrosis evaluation methods, such as Forn's index and AST-to-platelet ratio index.

CONCLUSION: LI is associated with the risk of HCC occurrence in hepatitis C patients. LI may be a substitute for liver biopsy when evaluating this risk and its combined use with Fib-4 is a better predictive method of HCC progression.

© 2014 Baishideng Publishing Group Inc. All rights reserved.

Key words: Ethoxibenzyl-magnetic resonance imaging; Hepatocellular carcinoma; Risk factor; Fibrosis

Abstract

AIM: To evaluate the efficacy of ethoxibenzyl-magnetic resonance imaging (EOB-MRI) as a predictor of hepatocellular carcinoma (HCC) development.

METHODS: Between August 2008 and 2009, we studied 142 hepatitis C virus-infected patients (male 70, female 72), excluding those with HCC or a past history, who underwent EOB-MRI in our hospital. The EOB-MRI index [liver-intervertebral disc ratio (LI)] was calculated as: (post-liver intensity/post-intervertebral disc intensity)/(pre-liver intensity/pre-intervertebral disc intensity).

RESULTS: The median follow-up period was 3.1 years and the patients were observed until the end of the study period (31 December, 2012). In the follow-up period, HCC occurred in 21 patients. The cumulative occurrence rates were 2.1%, 9.1%, and 14.1% at 1, 2, and 3 years, respectively. Using the optimal cut-off value of LI 1.46, on univariate analysis, age, aspartate amino transferase (AST), α -fetoprotein (AFP) ≥ 10 , albumin, total cholesterol, prothrombin time, platelets,

Core tip: This manuscript addresses a method of hepatocellular carcinoma (HCC) prediction by using a new technique that evaluates hepatic fibrosis using a non-invasive method (reported recently). This is the first reported study to consider a possible substitute for liver biopsy by using an magnetic resonance imaging (MRI) method (a widespread method in public medical services) for evaluating the risk of occurrence. We propose that this method will become one of the most popular and precise noninvasive methods to predict the occurrence of HCC, and the combination of this MRI method and Fib-4 index may provide a better predictive method of HCC progression.

Nojiri S, Fujiwara K, Shinkai N, Endo M, Joh T. Evaluation of hepatocellular carcinoma development in patients with chronic hepatitis C by EOB-MRI. *World J Hepatol* 2014; 6(12): 930-938 Available from: URL: <http://www.wjgnet.com/1948-5182/full/v6/i12/930.htm> DOI: <http://dx.doi.org/10.4254/wjh.v6.i12.930>

INTRODUCTION

The major cause of cirrhosis globally is chronic hepatitis C. The risk of hepatocellular carcinoma (HCC) development is related to this, as reported in several papers^[1-3], and advanced fibrosis increases the risk of carcinogenesis^[1]. The prognosis of HCC is not good, even when detected and treated at an early stage^[4-6]. Thus, it is important to determine outpatients' fibrotic stage in order to identify the risk of HCC occurrence in the management of patients with chronic liver disease. Even now, to determine the grade of fibrosis, the gold standard is liver biopsy, but it is associated with certain problems such as sample error and severe complications^[7-10]. Previously, noninvasive methods to evaluate fibrosis were reported, such as Forn's index^[11], the Fibro index^[12], and aspartate amino transferase-to-platelet ratio index (APRI)^[13]. Using laboratory data, it has been reported that the Fibrotest is a useful prognostic factor for hepatitis C patients^[14]. On the other hand, specific methods, such as transient elastography^[15], magnetic resonance (MR) elastography^[16], and acoustic radiation force impulse^[17], have been reported to evaluate fibrosis as surrogates of liver biopsy. Transient elastography is reported to indicate a wide-ranging risk of HCC incidence. We recently reported the accuracy of staging fibrosis in chronic hepatitis in hepatitis C virus (HCV) infection using ethoxibenzyl-MR imaging (EOB-MRI)^[18], but there are no reports about a predictor of HCC incidence using this new method. Here, we report a study to evaluate the efficacy of EOB-MRI as a predictor of HCC development.

MATERIALS AND METHODS

Patients

Between August 2008 and December 2009, we studied 142 HCV-infected patients, excluding those with HCC or a past history, who underwent EOB-MRI in our hospital. Clinical data were obtained within one month of EOB-MRI information being obtained. The definition of HCV infection was determined by a positive anti-HCV antibody and detection of quantitative or qualitative HCV RNA. Exclusion criteria were as follows: (1) infection with hepatitis B or human immunodeficiency viruses; (2) alcohol abuse; (3) the presence of numerous liver tumors; and (4) having previously undergone partial splenic arterial embolization or splenectomy. During the follow-up period, the history of interferon (IFN) therapies and associated responses was examined. We defined a sustained virological response (SVR) as undetectable HCV-RNA for at least 24 wk after IFN therapy. The study protocol conformed to the ethics guidelines of the 1975 Helsinki Declaration and was approved a priori by the institution's human research committee. All blood tests were performed within 1 wk before or after MRI.

Follow-up of patients and HCC diagnosis

The screening of HCC occurrence was carried out by

enhanced MRI or enhanced computed tomography (CT). Outpatients were followed up with blood tests, tumor markers for HCC, and image analysis, such as ultrasonography, enhanced CT, or enhanced MRI, every 3 to 6 mo. The diagnosis of HCC was determined by enhanced CT or enhanced MRI, considering enhancement in the arterial phase and washout in the earlier delayed venous phase as a classical sign of HCC^[19,20]. When the diagnosis of HCC was not clear in CT or MRI, a histological diagnosis was performed by tumor biopsy^[21]. Cases that were diagnosed as HCC within 6 mo from the first MRI trial were excluded because there should have been only small HCC when the first MRI was performed. This study was continued until December 31, 2012.

MRI techniques

A 1.5-Tesla MR system (Philips Co., Amsterdam, the Netherlands) was used: 0.025 mmol/kg body weight gadoxetate disodium was intravenously injected and quantitative measurements were performed using unenhanced and gadoxetate disodium-enhanced imaging at 20, 35, 70, and 180 s, and the imaging at 15, 20, and 25 min was obtained as hepatobiliary phases. Imaging parameters were as follows: repetition time/echo time = 4.17/2.05 ms. Then, 1-2 cm² regions of interest of the mean signal intensity value of the liver were measured. At each MRI, the means of three different regions of right anterior, right posterior, and left lateral segments of the liver devoid of large vessels or severe artifacts were calculated. Using the liver to intervertebral disk signal intensity (LISI) and liver signal intensity/intervertebral disk signal intensity, we calculated the post-enhanced LISI/pre-enhanced LISI [described as liver-intervertebral disc ratio (LI)], as detailed in our previous report^[18]. We used hepatobiliary phase data at 20 min because this is most commonly used globally and the data showed no significant difference from the value at 25 min. As we reported previously, because cut-off values of 1.31 and 1.80 are representative values of liver cirrhosis and significant fibrosis of the liver, we divided all patients into < 1.31, 1.311 to 1.38, 1.381 to 1.50, 1.501 to 1.60, and > 1.601. Age, sex, aspartate aminotransferase (AST), alanine aminotransferase (ALT), serum albumin level, total bilirubin (T.Bil), gamma-glutamyl transpeptidase (γ GTP), total cholesterol, and platelet count (Plt) were examined. The prothrombin time (PT) was measured as a percentage of the daily internal control.

Statistical analysis

Baseline data are presented as the mean \pm SD with the range in parentheses for quantitative variables. The best models derived from the categorical variables were compared by the χ^2 or Fisher's exact test, whereas Wilcoxon rank sum test (nonparametric) for continuous variables and the unpaired Student's *t* test (parametric) were used to evaluate differences in age, sex, albumin, T.Bil, PT, Plt, AST, ALT, γ GTP, total cholesterol, and α -fetoprotein (AFP) at the time of entry. The results are reported as

Table 1 Baseline characteristics of 142 patients with chronic hepatitis C

Variables	Mean ± SD
Age (yr)	66.1 ± 12.4 (28-87)
Male (M/F)	70/72
AST (U/L)	48.9 ± 23.4 (11-155)
ALT (U/L)	51.7 ± 34.1 (10-228)
Serum albumin (g/dL)	4.1 ± 0.5 (2.4-5)
Gamma-GT(IU/L)	67 ± 92 (14-811)
ALP (U/L)	331 ± 171 (141-1206)
T.Chol (mg/dL)	175 ± 36 (90-280)
T.Bil (mg/dL)	0.86 ± 0.42 (0.3-2.9)
PT (%)	93 ± 15.2 (55.2-134)
Platelet (× 10 ³ /μL)	136 ± 60 (42-338)
AFP (ng/mL)	14.5 ± 27.5 (1.6-235)
LI	1.51 ± 0.19 (1.11-2.15)
Patients who received IFN, <i>n</i> (%)	39 (27.5)
Patients who achieved SVR, <i>n</i> (%)	27 (19.0)

AST: Aspartate amino transferase; ALT: Alanine aminotransferase; Gamma-GT: Gamma-glutamyl transpeptidase; T.Chol: Total cholesterol; T.Bil: Total bilirubin; PT: Prothrombin time; AFP: α-fetoprotein; LI: Liver-intervertebral disc ratio; IFN: Interferon; SVR: Sustained virologic response; ALP: Alkaline phosphatase; F: Female; M: Male.

hazard ratios with 95%CI. *P* < 0.05 in a two-tailed test was considered significant for all analyses. Patients were censored when they died without HCC development, when they stopped visiting, or when the study period ended. Cumulative occurrence curves were analyzed using the Kaplan-Meier method and tested by Wilcoxon's method. The Cox proportional hazard regression model was used to estimate the risk factors for hepatocarcinogenesis using the following variables in univariate and multivariate analyses: sex, albumin, T.Bil, PT, Plt, AST, ALT, γGTP, alkaline phosphatase (ALP), total cholesterol, AFP (≥ 10 ng/mL), LI (< 1.46) at the time of entry, and the history of IFN therapy (with or without, and SVR or non-SVR).

All statistical analyses were performed using IBM SPSS Statistics 21 software (IBM, Chicago, IL, United States).

RESULTS

Patient characteristics

A total of 145 patients who had undergone EOB-MRI were examined. Three patients were excluded because they developed HCC within 6 mo.

Patient characteristics at the time of EOB-MRI are shown in Table 1. There were 70 men and 72 women, with a mean age of 66.1 ± 12.4 years. The mean AFP level was 14.5 ng/mL and the median was 5 ng/mL. Thirty-seven patients (26%) had an AFP level of ≥ 10. Thirty-nine patients received IFN and 27 patients achieved SVR in the follow-up period.

Occurrence of HCC and patient follow-up

The median follow-up period was 3.1 years, during which 14 (9.8%) patients were lost to follow-up and were cen-

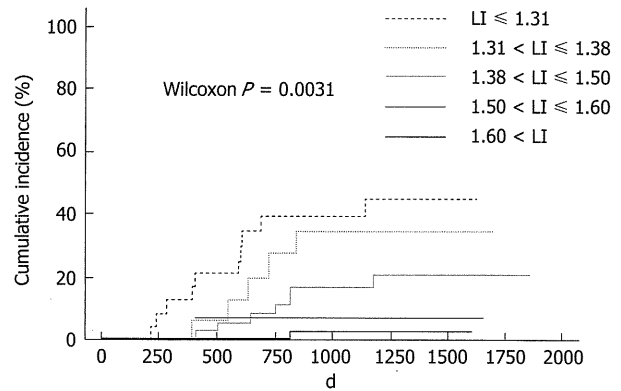


Figure 1 Cumulative incidence of hepatocellular carcinoma occurrence stratified by liver-intervertebral disc ratio. Cumulative occurrence rates increased gradually in an LI-independent manner. LI: Liver-intervertebral disc ratio.

sored at the time of the last visit. Nine patients died of liver failure, one died of gastroenterological varices rupture, and nine died of liver-unrelated causes, and they were censored when they died. The remaining patients were observed until the end of the study period (31 December, 2012). During the follow-up period, HCC occurred in 21 patients. The cumulative HCC occurrence rates were 2.1%, 9.1%, and 14.1% at 1, 2, and 3 years, respectively, by the Kaplan-Meier method. Baseline characteristics were compared in patients with and without HCC occurrence (Table 2). There were no significant differences between the no-HCC occurrence group and the HCC occurrence group in terms of age, sex, ALT level, gamma-GT, T.Bil, the performance of IFN therapy, and the achievement of SVR, while AST, ALP, and AFP were higher and albumin, total cholesterol (T.Chol), PT, platelets, and LI were lower in the HCC occurrence group than in the no-HCC occurrence group.

Occurrence rate of HCC stratified by LI

The cumulative occurrence rates at 1, 2, and 3 years in each LI group were 0%, 0%, and 2% in patients with LI ≥ 1.60; 0%, 5.8%, and 5.8% in patients with LI 1.501-1.600; 0%, 7.1%, and 14.3% in patients with LI 1.381-1.500; 0%, 11.8%, and 23.5% in patients with LI 1.311-1.380; and 12.5%, 29.2%, and 33.3% in patients with LI ≤ 1.310, respectively (Figure 1). The occurrence rates differed significantly among the 5 LI groups (*P* = 0.0031), increasing with decreasing LI.

The receiver operating characteristic curve (ROC) curve was used to evaluate the cumulative incidence of LI and a cut-off value of 1.46 was determined [area under the ROC (AUROC): 0.765 ± 0.05, 0.669-0.861] by calculating the highest accuracy value (0.63) and likelihood ratio (2.19). The use of this cut-off value resulted in sensitivity: 90.5%, specificity: 58.7%, positive predictive value: 27.5%, and negative predictive value: 97.3%. We compared these results with several representative fibrosis evaluation methods reported previously (Figure 2). The AUROC for each was: Forn's index, 0.733 ± 0.05,

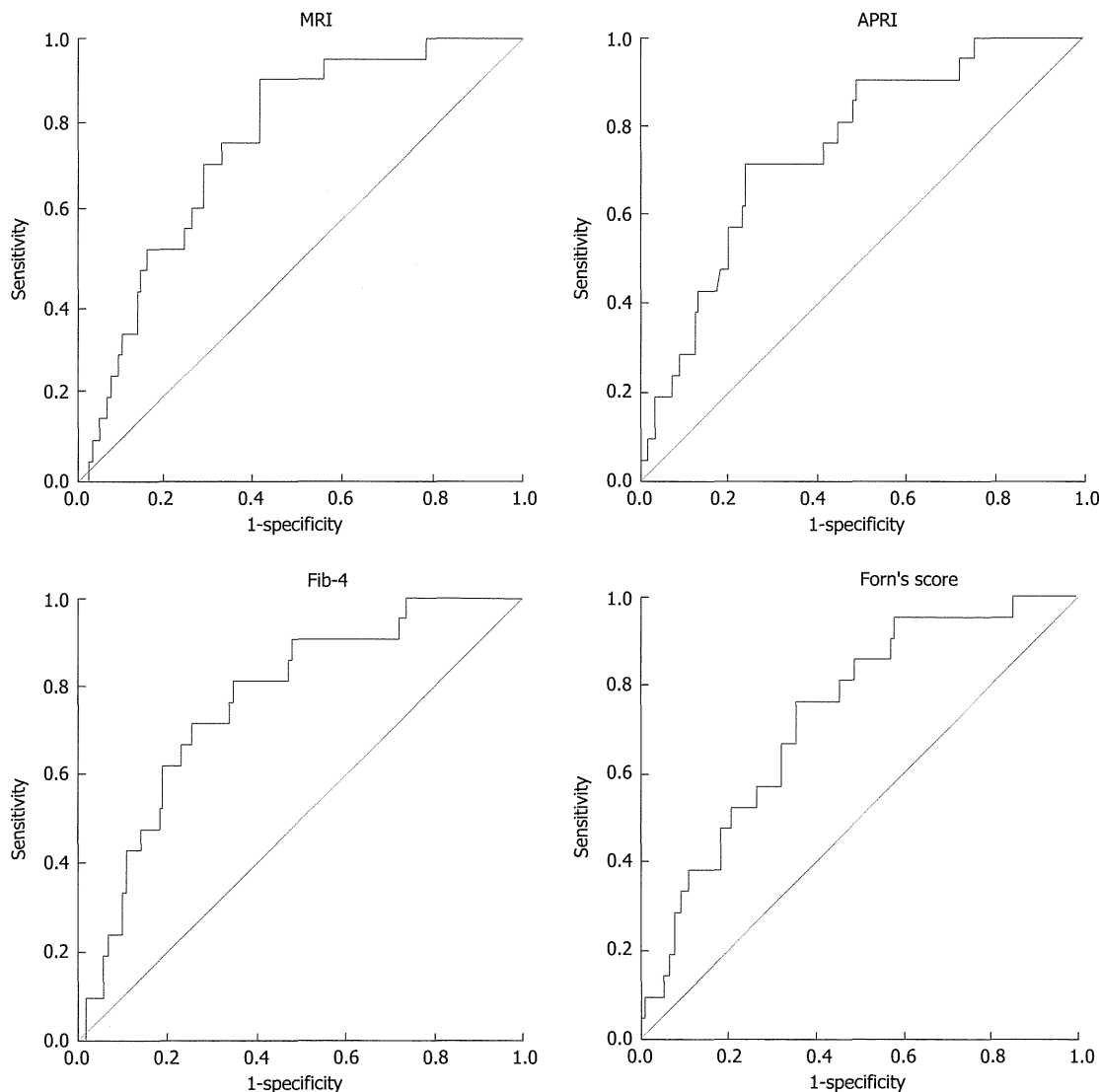


Figure 2 Receiver operating characteristic curve evaluating the cumulative incidence of liver-intervertebral disc ratio, aspartate amino transferase-to-platelet ratio index, Fib-4, and Forn's index. APRI: aspartate amino transferase-to-platelet ratio index; MRI: Magnetic resonance imaging.

Table 2 Comparison of baseline characteristics between patients who have no hepatocellular carcinoma occurrence and hepatocellular carcinoma occurrence

Variables	No HCC occurrence <i>n</i> = 121	HCC occurrence <i>n</i> = 21	<i>P</i> value
Age (yr)	65.4 ± 12.9 (28-87)	70.3 ± 7.9 (51-79)	0.094
Sex (M/F)	59/62	11/10	0.759
AST (U/L)	46.0 ± 20.4 (11-110)	65.5 ± 31.6 (34-155)	0.000
ALT (U/L)	49.5 ± 32.5 (10-228)	64.4 ± 40.5 (31-205)	0.063
Serum albumin (g/dL)	4.1 ± 0.5 (2.4-5)	3.8 ± 0.5 (2.6-4.7)	0.030
Gamma-GT (IU/L)	67 ± 97 (14-811)	62 ± 43 (16-226)	0.829
ALP (U/L)	315 ± 158 (141-1206)	426 ± 212 (150-1006)	0.006
T.Chol (mg/dL)	178 ± 36 (90-280)	159 ± 35 (93-260)	0.029
T.Bil (mg/dL)	0.86 ± 0.42 (0.3-2.9)	0.86 ± 0.42 (0.3-2.9)	0.287
PT (%)	94 ± 15.5 (55.2-134)	86.8 ± 12.0 (67-110)	0.045
Platelet (× 10 ³ /μL)	142 ± 61 (42-338)	104 ± 40 (46-166)	0.006
AFP (ng/mL)	11.7 ± 26.3 (1.6-235)	30.3 ± 31.6 (4.2-116)	0.004
LI	1.53 ± 0.20 (1.11-2.15)	1.37 ± 0.10 (1.23-1.67)	0.000
Patients who received IFN, <i>n</i> (%)	37 (30.6)	2 (9.5)	0.062
Patients who achieved SVR, <i>n</i> (%)	25 (20.7)	2 (9.5)	0.366

HCC: Hepatocellular carcinoma; AST: Aspartate amino transferase; ALT: Alanine aminotransferase; Gamma-GT: Gamma-glutamyl transpeptidase; ALP: Alkaline phosphatase; T.Chol: Total cholesterol; T.Bil: Total bilirubin; PT: Prothrombin time; AFP: α-fetoprotein; LI: Liver-intervertebral disc ratio; IFN: Interferon; SVR: Sustained virologic response; F: Female; M: Male.

Table 3 Risk factors contributing to hepatocellular carcinoma incidence

Variable	Univariate analysis			Multivariate analysis		
	Risk ratio	95%CI	P-Value	Risk ratio	95%CI	P-Value
Age (per 1 year old)	1.04	1.01-1.09	0.045	1.05	0.99-1.11	0.139
Sex (F)	0.74	0.31-1.73	0.483			
AST (U/L)	1.02	1.01-1.03	< 0.001	1.01	0.99-1.03	0.200
ALT (U/L)	1.01	0.99-1.02	0.12			
Serum albumin (g/dL)	0.27	0.12-0.60	0.001	0.62	0.17-2.26	0.469
Gamma-GT (IU/L)	1.00	0.99-1.01	0.942			
ALP (U/L)	1.002	1.001-1.004	0.006	1.00	0.99-1.01	0.504
T.Chol (mg/dL)	0.98	0.97-0.99	0.01	0.99	0.98-1.01	0.483
T.Bil (mg/dL)	2.01	0.77-5.25	0.153			
PT (%)	0.97	0.94-0.99	0.018	1.01	0.97-1.05	0.621
Platelet ($\times 10^3/\mu\text{L}$)	0.98	0.97-0.99	0.003	0.99	0.98-1.01	0.281
AFP (≥ 10 ng/mL)	7.39	2.97-18.37	< 0.001	3.10	1.03-9.35	0.045
LI (< 1.46)	11.63	2.71-49.9	0.001	6.05	1.34-27.3	0.019
≥ 1.601	1.00					
1.501 to 1.60	2.68	0.17-42.9	0.48			
1.381 to 1.50	7.24	0.89-58.9	0.06			
1.311 to 1.38	11.5	1.2-103	0.02			
≤ 1.31	17.34	2.16-138.7	0.007			
Patients who received IFN	0.20	0.04-0.87	0.032	1.09	0.21-5.62	0.917
Patients who achieved SVR	0.35	0.81-1.51	0.158			

AST: Aspartate amino transferase; ALT: Alanine aminotransferase; Gamma-GT: Gamma-glutamyl transpeptidase; ALP: Alkaline phosphatase; T.Chol: Total cholesterol; T.Bil: Total bilirubin; PT: Prothrombin time; AFP: α -fetoprotein; LI: Liver-intervertebral disc ratio; IFN: Interferon; SVR: Sustained virologic response; F: Female.

Table 4 Analyses of liver-intervertebral disc ratio contributions to hepatocellular carcinoma occurrence risk divided by other risk factors

	Subgroup	n	Risk ratio	95%CI	P-Value
Age	≥ 69	75	12.51	1.63-95.82	0.015
	< 69	67	9.2	1.11-76.58	0.041
Sex	Male	70	8.4	1.08-65.18	0.042
	Female	72	7.024	1.49-33.14	0.014
Platelet ($\times 10^3/\mu\text{L}$)	< 120	67	4.48	1.01-19.89	0.048
	≥ 120	75	14.96	1.89-118.2	0.013
Albumin (g/dL)	< 4.2	72	9.7	1.27-74.24	0.029
	≥ 4.2	70	10.79	1.29-89.7	0.028
ALT (U/L)	≥ 50	88	10.98	1.39-86.7	0.023
	< 50	54	12.7	1.62-99.63	0.016
IFN	-	103	13.35	1.78-100.1	0.011
	+	39	3.498	0.22-55.96	0.376
SVR	-	115	15.98	2.13-119.7	0.007
	+	27	3.795	0.28-60.74	0.346

ALT: Alanine aminotransferase; IFN: Interferon; SVR: Sustained virologic response.

0.627-0.840; APRI, 0.752 ± 0.05 , 0.648-0.856; and Fib-4, 0.765 ± 0.05 , 0.665-0.861. Comparing these results, MRI is as effective as the Fib-4 method and more effective than Forn's index and APRI.

Prognostic Factors of HCC occurrence risk by univariate and multivariate analyses

On univariate analysis, LI < 1.46, AFP ≥ 10 , age (per year of age), AST (per 1 U/L), serum albumin (per 1 g/dL), ALP (per 1 U/L), T.Chol (per 1 mg/dL), PT (per 1%), platelets (per 1 $\times 10^3/\mu\text{L}$), and receiving IFN were identified as risk factors for the occurrence of HCC. The risk of HCC occurrence increased in accordance with LI decrease. On multivariate analysis, LI < 1.46 ($P =$

0.019) and AFP ≥ 10 ng/mL ($P = 0.045$) were identified as independent factors; LI: risk ratio: 6.05 (1.34-27.3, $P = 0.019$) and AFP: 3.1 (1.03-9.35, $P = 0.045$) (Table 3). The LI contributions to HCC occurrence risk were also evaluated in subgroup analyses. We investigated whether higher LI was a significant risk factor with several other factors (Table 4). High LI was a significant risk factor even with low or high values of age, Plt, albumin, ALT, and male or not, IFN-treated or not, and SVR achieved or not. The LI contribution was greater at age ≥ 69 (older group) and with platelets $\geq 120 \times 10^3/\mu\text{L}$ (less fibrosis). In the IFN-untreated group and the SVR-unachieved group, there was a significant risk in low LI, but in the IFN-treated group and SVR not-achieved group, there

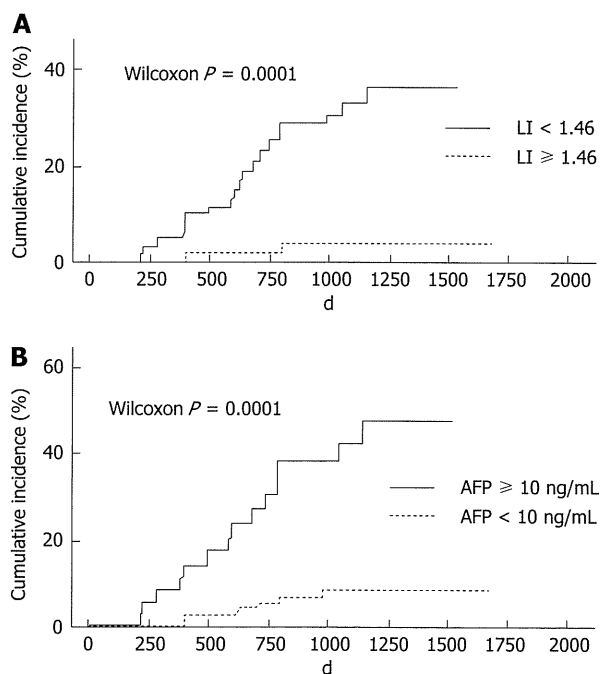


Figure 3 Relationship between cumulative occurrence rates and liver-intervertebral disc ratio (A), cumulative occurrence rates and serum α -fetoprotein level (B). A: Occurrence rates with LI < 1.46 were significantly higher than those with LI \geq 1.46; B: Occurrence rates with serum AFP \geq 10 ng/mL were significantly higher than in those with serum AFP < 10 ng/mL. LI: Liver-intervertebral disc ratio; AFP: α -fetoprotein.

were no significant differences because the sample numbers were very small.

Relationship between occurrence rate and LI or AFP

The occurrence rate in patients with LI < 1.46 was significantly higher than in those with LI \geq 1.46 (Wilcoxon $P < 0.0001$) (Figure 3A); in addition, in those with serum AFP \geq 10 ng/mL, it was significant higher than in those with serum AFP < 10 ng/mL (Wilcoxon $P < 0.0001$) (Figure 3B).

DISCUSSION

It is known that liver fibrosis is the strongest prognostic factor of chronic liver disease and liver biopsy is now recognized as the best method for evaluating this condition^[22], although it has problems such as complications. Several risk factors for HCC occurrence or recurrence have been reported, such as age, sex^[1], serum albumin level^[23,24], AFP level^[25], and high transaminase^[25]. Our study showed almost the same results as these previous reports. In particular, the progression of fibrosis may increase the risk of HCC incidence, so it is very important to determine the stage of liver damage^[26,27]. Various methods have been reported for the evaluation of liver fibrosis and have been divided into two groups: ultrasonographic methods^[15,17,28,29] and others^[16,18]. Although gadolinium ethoxybenzyl diethylene triamine pentaacetic acid (Gd-EOB-DTPA)-enhanced MRI is one of the most

sensitive methods to detect HCC development, it is also a very important method to evaluate liver fibrosis as a noninvasive investigation^[19,30]. We used Gd-EOB-DTPA-enhanced MRI and the LI:EOB-MRI index = (post-liver intensity/post-disc intensity)/(pre-liver intensity/pre-disc intensity) because it has the highest accuracy of all of the calculation methods using EOB-MRI^[18]. In this study, we used the 20-min hepatobiliary phase because many institutions accept the hepatobiliary phase as being 20 min after injection and it has also been accepted by consensus of the International Forum for Liver MRI^[31]. In our previous study, the data between 20 and 25 min showed no significant difference (data not shown).

LI constantly decreased as the fibrosis stage progressed to a higher stage, but many values overlapped between close fibrous stages, so we decided that the best cut-off point was 1.46 on the ROC curve by calculating the accuracy value and likelihood ratio. Using this cut-off value, LI < 1.46 always showed a high risk, with both low and high risks for several other factors, showing that lower LI is a strong independent risk factor and can complement other risk factors. LI may reflect not only the fibrosis stage but also functional aspects of the liver because it is decided by various factors, such as decreased hepatocytes, deficient hepatocyte function, and indocyanine green clearance^[32-34]. The uptake and excretion of gadoxetate disodium are carried out by the anion-transporting polypeptides Oatp1 and Mrp2^[35]. The balance of these effects may regulate the signal intensity of liver parenchyma in the hepatobiliary phase followed by a decrease of its signal upon hepatic damage or deteriorating cirrhosis^[36-38]. Viewed from this perspective, LI could be an outstanding predictor that reflects the occurrence of HCC and prognosis, in comparison to other methods that can assess only fibrosis.

In the present study, two patients developed HCC in the higher-LI group. According to their clinical data, both had significant splenomegaly and varices, and their actual pathology obtained from surgery was F4. OATP1B1/1B3 are hepatocyte-specific transporters determining the uptake of Gd-EOB-DTPA during MR, and genetic polymorphisms of their polypeptides might influence hepatic enhancement^[39], but their actual influence is relatively small and the intensity in the second case was extremely high, so it was thought to be difficult to explain this discrepancy completely. In particular, one of the two patients achieved SVR during observation but developed HCC. AFP of the two patients did not change even when HCC developed. The occurrence of HCC after IFN therapy is a rare but important problem, as some studies have reported recently^[40,41]. Chang *et al*^[40] advocated calculating the HCC prediction score after IFN therapy and, using this method, the score of our case was 5 in the so-called medium-risk group. Because the AUROC value of Fib-4 is as high as that of LI, the cut-off value (4.0) of Fib-4 was determined because the highest accuracy (0.669) was obtained, with sensitivity: 80.9%, specificity:

64.5%, positive predictive value: 28.3%, and negative predictive value: 95.1%. Using this cut-off value, 4 patients developed HCC at < 4. Interestingly, although LI and Fib-4 have similar ROC, there are relatively weak correlations between these two methods (Pearson, $r = -0.303$, $P = 0.0002$), so it is thought that they complement each other. Our two cases in which HCC development initially could not be predicted were finally predicted using Fib-4. Therefore, a combination of these two methods is a better predictive method than using a single predictive method as they complement each other and, in addition to information on clinical advanced liver fibrosis, such as low Plt, splenomegaly, and the existence of obvious varices, they will enable more accurate prediction of HCC progression.

Methods such as LI using EOB-MRI and transient elastography may be strong predictors of the HCC occurrence risk. Fibroscan is more cost-effective than MRI, but the equipment is very expensive and is restricted for use in specific hospitals because it can be used only to evaluate tissue elasticity and is ineffective in patients who are obese or have ascites. On the other hand, MRI can evaluate patients who have ascites and/or are obese and is used in many general hospitals, so it is a widely available method.

Our study revealed that the EOB-MRI index is associated with the risk of HCC occurrence in hepatitis C patients and may become a substitute for liver biopsy when evaluating the risk in these patients, even when their condition is not appropriate for other noninvasive methods, and the combination of EOB-MRI index and Fib-4 may become a better predictive method of HCC progression.

COMMENTS

Background

The major cause of cirrhosis is chronic hepatitis C and it is well known that the risk of occurrence of hepatocellular carcinoma increases as fibrosis progresses. Therefore, it is important to reveal the fibrosis stages of outpatients.

Research frontiers

The gold standard test to investigate the fibrous stage of the liver is needle biopsy, but it is potentially harmful, so other noninvasive methods are needed and several have been reported.

Innovations and breakthroughs

This method can predict the hepatocellular carcinoma (HCC) incidence noninvasively and has the advantage of being suitable for some individuals for whom other methods are unavailable due to several factors, such as the presence of ascites.

Applications

This method uses pictures that are typically obtained to detect HCC in outpatients, so it does not require the preparation of special equipment.

Peer review

The authors evaluated the development of HCC in hepatitis C virus patients using ethoxibenzyl-magnetic resonance imaging (EOM-MRI), and observed that EOM-MRI is a highly sensitive and predictive method. This study was well performed, and the manuscript is overall well written and easy to understand.

ACKNOWLEDGMENTS

We thank all of the doctors who participated in this study.

REFERENCES

- 1 **Yoshida H**, Shiratori Y, Moriyama M, Arakawa Y, Ide T, Sata M, Inoue O, Yano M, Tanaka M, Fujiyama S, Nishiguchi S, Kuroki T, Imazeki F, Yokosuka O, Kinoyama S, Yamada G, Omata M. Interferon therapy reduces the risk for hepatocellular carcinoma: national surveillance program of cirrhotic and noncirrhotic patients with chronic hepatitis C in Japan. IHIT Study Group. Inhibition of Hepatocarcinogenesis by Interferon Therapy. *Ann Intern Med* 1999; **131**: 174-181 [PMID: 10428733 DOI: 10.7326/0003-4819-131-3-199908030-00003]
- 2 **Tsukuma H**, Hiyama T, Tanaka S, Nakao M, Yabuuchi T, Kitamura T, Nakanishi K, Fujimoto I, Inoue A, Yamazaki H. Risk factors for hepatocellular carcinoma among patients with chronic liver disease. *N Engl J Med* 1993; **328**: 1797-1801 [PMID: 7684822 DOI: 10.1056/NEJM199306243282501]
- 3 **Ikeda K**, Saitoh S, Koida I, Arase Y, Tsubota A, Chayama K, Kumada H, Kawanishi M. A multivariate analysis of risk factors for hepatocellular carcinogenesis: a prospective observation of 795 patients with viral and alcoholic cirrhosis. *Hepatology* 1993; **18**: 47-53 [PMID: 7686879 DOI: 10.1002/hep.1840180109]
- 4 **Cottone M**, Turri M, Caltagirone M, Parisi P, Orlando A, Fiorentino G, Virdone R, Fusco G, Grasso R, Simonetti RG. Screening for hepatocellular carcinoma in patients with Child's A cirrhosis: an 8-year prospective study by ultrasound and alpha-fetoprotein. *J Hepatol* 1994; **21**: 1029-1034 [PMID: 7535323 DOI: 10.1016/S0168-8278(05)80613-0]
- 5 **Oka H**, Kurioka N, Kim K, Kanno T, Kuroki T, Mizoguchi Y, Kobayashi K. Prospective study of early detection of hepatocellular carcinoma in patients with cirrhosis. *Hepatology* 1990; **12**: 680-687 [PMID: 1698703 DOI: 10.1002/hep.1840120411]
- 6 **Zoli M**, Magalotti D, Bianchi G, Gueli C, Marchesini G, Pisi E. Efficacy of a surveillance program for early detection of hepatocellular carcinoma. *Cancer* 1996; **78**: 977-985 [PMID: 8780534]
- 7 **Bedossa P**, Dargère D, Paradis V. Sampling variability of liver fibrosis in chronic hepatitis C. *Hepatology* 2003; **38**: 1449-1457 [PMID: 14647056 DOI: 10.1016/j.hep.2003.09.022]
- 8 **Perrault J**, McGill DB, Ott BJ, Taylor WF. Liver biopsy: complications in 1000 inpatients and outpatients. *Gastroenterology* 1978; **74**: 103-106 [PMID: 618417]
- 9 **Wong JB**, Koff RS. Watchful waiting with periodic liver biopsy versus immediate empirical therapy for histologically mild chronic hepatitis C. A cost-effectiveness analysis. *Ann Intern Med* 2000; **133**: 665-675 [PMID: 11074899 DOI: 10.7326/0003-4819-133-9-200011070-00008]
- 10 **Rockey DC**, Caldwell SH, Goodman ZD, Nelson RC, Smith AD. Liver biopsy. *Hepatology* 2009; **49**: 1017-1044 [PMID: 19243014 DOI: 10.1002/hep.22742]
- 11 **Forns X**, Ampurdanès S, Llovet JM, Aponte J, Quintó L, Martínez-Bauer E, Bruguera M, Sánchez-Tapias JM, Rodés J. Identification of chronic hepatitis C patients without hepatic fibrosis by a simple predictive model. *Hepatology* 2002; **36**: 986-992 [PMID: 12297848 DOI: 10.1053/jhep.2002.36128]
- 12 **Koda M**, Matunaga Y, Kawakami M, Kishimoto Y, Suou T, Murawaki Y. FibroIndex, a practical index for predicting significant fibrosis in patients with chronic hepatitis C. *Hepatology* 2007; **45**: 297-306 [PMID: 17256741 DOI: 10.1002/hep.21520]
- 13 **Wai CT**, Greenson JK, Fontana RJ, Kalbfleisch JD, Marrero JA, Conjeevaram HS, Lok AS. A simple noninvasive index can predict both significant fibrosis and cirrhosis in patients with chronic hepatitis C. *Hepatology* 2003; **38**: 518-526 [PMID: 12883497 DOI: 10.1053/jhep.2003.50346]
- 14 **Ngo Y**, Munteanu M, Messous D, Charlotte F, Imbert-Bismut F, Thabut D, Lebray P, Thibault V, Benhamou Y, Moussalli J, Ratzju V, Poynard T. A prospective analysis of the prognos-

- tic value of biomarkers (FibroTest) in patients with chronic hepatitis C. *Clin Chem* 2006; **52**: 1887-1896 [PMID: 16931569 DOI: 10.1373/clinchem.2006.070961]
- 15 **Castéra L**, Vergniol J, Foucher J, Le Bail B, Chanteloup E, Haaser M, Darriet M, Couzigou P, De Ledinghen V. Prospective comparison of transient elastography, Fibrotest, APRI, and liver biopsy for the assessment of fibrosis in chronic hepatitis C. *Gastroenterology* 2005; **128**: 343-350 [PMID: 15685546 DOI: 10.1053/j.gastro.2004.11.018]
 - 16 **Rouvière O**, Yin M, Dresner MA, Rossman PJ, Burgart LJ, Fidler JL, Ehman RL. MR elastography of the liver: preliminary results. *Radiology* 2006; **240**: 440-448 [PMID: 16864671 DOI: 10.1148/radiol.2402050606]
 - 17 **Rizzo L**, Calvaruso V, Cacopardo B, Alessi N, Attanasio M, Petta S, Fatuzzo F, Montineri A, Mazzola A, L'abbate L, Nunnari G, Bronte F, Di Marco V, Craxi A, Cammà C. Comparison of transient elastography and acoustic radiation force impulse for non-invasive staging of liver fibrosis in patients with chronic hepatitis C. *Am J Gastroenterol* 2011; **106**: 2112-2120 [PMID: 21971536 DOI: 10.1038/ajg.2011.341]
 - 18 **Nojiri S**, Kusakabe A, Fujiwara K, Shinkai N, Matsuura K, Iio E, Miyaki T, Joh T. Noninvasive evaluation of hepatic fibrosis in hepatitis C virus-infected patients using ethoxybenzyl-magnetic resonance imaging. *J Gastroenterol Hepatol* 2013; **28**: 1032-1039 [PMID: 23432660 DOI: 10.1111/jgh.12181]
 - 19 **Bruix J**, Sherman M. Management of hepatocellular carcinoma. *Hepatology* 2005; **42**: 1208-1236 [PMID: 16250051 DOI: 10.1002/hep.20933]
 - 20 **Torzilli G**, Minagawa M, Takayama T, Inoue K, Hui AM, Kubota K, Ohtomo K, Makuuchi M. Accurate preoperative evaluation of liver mass lesions without fine-needle biopsy. *Hepatology* 1999; **30**: 889-893 [PMID: 10498639 DOI: 10.1002/hep.510300411]
 - 21 **Edmondson HA**, Steiner PE. Primary carcinoma of the liver: a study of 100 cases among 48,900 necropsies. *Cancer* 1954; **7**: 462-503 [PMID: 13160935]
 - 22 **Dienstag JL**. The role of liver biopsy in chronic hepatitis C. *Hepatology* 2002; **36**: S152-S160 [PMID: 12407589 DOI: 10.1002/hep.1840360720]
 - 23 **Ikeda K**, Saitoh S, Suzuki Y, Kobayashi M, Tsubota A, Koida I, Arase Y, Fukuda M, Chayama K, Murashima N, Kumada H. Disease progression and hepatocellular carcinogenesis in patients with chronic viral hepatitis: a prospective observation of 2215 patients. *J Hepatol* 1998; **28**: 930-938 [PMID: 9672166 DOI: 10.1016/S0168-8278(98)80339-5]
 - 24 **Nojiri S**, Kusakabe A, Shinkai N, Matsuura K, Iio E, Miyaki T, Joh T. Factors influencing distant recurrence of hepatocellular carcinoma following combined radiofrequency ablation and transarterial chemoembolization therapy in patients with hepatitis C. *Cancer Manag Res* 2011; **3**: 267-272 [PMID: 21847355 DOI: 10.2147/CMR.S22073]
 - 25 **Inoue A**, Tsukuma H, Oshima A, Yabuuchi T, Nakao M, Matsunaga T, Kojima J, Tanaka S. Effectiveness of interferon therapy for reducing the incidence of hepatocellular carcinoma among patients with type C chronic hepatitis. *J Epidemiol* 2000; **10**: 234-240 [PMID: 10959605 DOI: 10.2188/jea.10.234]
 - 26 **El-Serag HB**, Rudolph KL. Hepatocellular carcinoma: epidemiology and molecular carcinogenesis. *Gastroenterology* 2007; **132**: 2557-2576 [PMID: 17570226 DOI: 10.1053/j.gastro.2007.04.061]
 - 27 **Fattovich G**, Stroffolini T, Zagni I, Donato F. Hepatocellular carcinoma in cirrhosis: incidence and risk factors. *Gastroenterology* 2004; **127**: S35-S50 [PMID: 15508101]
 - 28 **Masuzaki R**, Tateishi R, Yoshida H, Goto E, Sato T, Ohki T, Imamura J, Goto T, Kanai F, Kato N, Ikeda H, Shiina S, Kawabe T, Omata M. Prospective risk assessment for hepatocellular carcinoma development in patients with chronic hepatitis C by transient elastography. *Hepatology* 2009; **49**: 1954-1961 [PMID: 19434742 DOI: 10.1002/hep.22870]
 - 29 **Yada N**, Kudo M, Morikawa H, Fujimoto K, Kato M, Kawada N. Assessment of liver fibrosis with real-time tissue elastography in chronic viral hepatitis. *Oncology* 2013; **84 Suppl 1**: 13-20 [PMID: 23428853 DOI: 10.1159/000345884]
 - 30 **Watanabe H**, Kanematsu M, Goshima S, Kondo H, Onozuka M, Moriyama N, Bae KT. Staging hepatic fibrosis: comparison of gadoxetate disodium-enhanced and diffusion-weighted MR imaging--preliminary observations. *Radiology* 2011; **259**: 142-150 [PMID: 21248234]
 - 31 **Tanimoto A**, Lee JM, Murakami T, Huppertz A, Kudo M, Grazioli L. Consensus report of the 2nd International Forum for Liver MRI. *Eur Radiol* 2009; **19 Suppl 5**: S975-S989 [PMID: 19851766 DOI: 10.1007/s00330-009-1624-y]
 - 32 **Motosugi U**, Ichikawa T, Tominaga L, Sou H, Sano K, Ichikawa S, Araki T. Delay before the hepatocyte phase of Gd-EOB-DTPA-enhanced MR imaging: is it possible to shorten the examination time? *Eur Radiol* 2009; **19**: 2623-2629 [PMID: 19471935 DOI: 10.1007/s00330-009-1467-6]
 - 33 **Tschirch FT**, Struwe A, Petrowsky H, Kakales I, Marincek B, Weishaupt D. Contrast-enhanced MR cholangiography with Gd-EOB-DTPA in patients with liver cirrhosis: visualization of the biliary ducts in comparison with patients with normal liver parenchyma. *Eur Radiol* 2008; **18**: 1577-1586 [PMID: 18369632 DOI: 10.1007/s00330-008-0929-6]
 - 34 **Ryeom HK**, Kim SH, Kim JY, Kim HJ, Lee JM, Chang YM, Kim YS, Kang DS. Quantitative evaluation of liver function with MRI Using Gd-EOB-DTPA. *Korean J Radiol* 2004; **5**: 231-239 [PMID: 15637473 DOI: 10.3348/kjr.2004.5.4.231]
 - 35 **van Montfoort JE**, Stieger B, Meijer DK, Weinmann HJ, Meier PJ, Fattinger KE. Hepatic uptake of the magnetic resonance imaging contrast agent gadoxetate by the organic anion transporting polypeptide Oatp1. *J Pharmacol Exp Ther* 1999; **290**: 153-157 [PMID: 10381771]
 - 36 **Nakai K**, Tanaka H, Hanada K, Ogata H, Suzuki F, Kumada H, Miyajima A, Ishida S, Sunouchi M, Habano W, Kamikawa Y, Kubota K, Kita J, Ozawa S, Ohno Y. Decreased expression of cytochromes P450 1A2, 2E1, and 3A4 and drug transporters Na⁺-taurocholate-cotransporting polypeptide, organic cation transporter 1, and organic anion-transporting peptide-C correlates with the progression of liver fibrosis in chronic hepatitis C patients. *Drug Metab Dispos* 2008; **36**: 1786-1793 [PMID: 18515332 DOI: 10.1124/dmd.107.020073]
 - 37 **Ogasawara K**, Terada T, Katsura T, Hatano E, Ikai I, Yamakawa Y, Inui K. Hepatitis C virus-related cirrhosis is a major determinant of the expression levels of hepatic drug transporters. *Drug Metab Pharmacokinet* 2010; **25**: 190-199 [PMID: 20460825 DOI: 10.2133/dmpk.25.190]
 - 38 **Hinoshita E**, Taguchi K, Inokuchi A, Uchiumi T, Kinukawa N, Shimada M, Tsuneyoshi M, Sugimachi K, Kuwano M. Decreased expression of an ATP-binding cassette transporter, MRP2, in human livers with hepatitis C virus infection. *J Hepatol* 2001; **35**: 765-773 [PMID: 11738104 DOI: 10.1007/s11605-011-1484-z]
 - 39 **Okubo H**, Ando H, Kokubu S, Miyazaki A, Watanabe S, Fujimura A. Polymorphisms in the organic anion transporting polypeptide genes influence liver parenchymal enhancement in gadoxetic acid-enhanced MRI. *Pharmacogenomics* 2013; **14**: 1573-1582 [PMID: 24088128 DOI: 10.2217/pgs.13.132]
 - 40 **Chang KC**, Wu YY, Hung CH, Lu SN, Lee CM, Chiu KW, Tsai MC, Tseng PL, Huang CM, Cho CL, Chen HH, Hu TH. Clinical-guide risk prediction of hepatocellular carcinoma development in chronic hepatitis C patients after interferon-based therapy. *Br J Cancer* 2013; **109**: 2481-2488 [PMID: 24084770 DOI: 10.1038/bjc.2013.564]
 - 41 **Izumi N**, Asahina Y, Kurosaki M, Yamada G, Kawai T, Kajiwara E, Okamura Y, Takeuchi T, Yokosuka O, Kariyama K, Toyoda J, Inao M, Tanaka E, Moriwaki H, Adachi H,

Nojiri S *et al.* Evaluation of HCC development by EOB-MRI

Katsushima S, Kudo M, Takaguchi K, Hiasa Y, Chayama K, Yatsunami H, Oketani M, Kumada H. Inhibition of hepatocellular carcinoma by PegIFN α -2a in patients with

chronic hepatitis C: a nationwide multicenter cooperative study. *J Gastroenterol* 2013; **48**: 382-390 [PMID: 22875473 DOI: 10.1007/s00535-012-0641-9]

P-Reviewer: Chua MS **S-Editor:** Gong XM
L-Editor: A **E-Editor:** Liu SQ



Hepatic Congestion Leads to Fibrosis: Findings in a Newly Developed Murine Model

See Article on Page 648

Passive hepatic congestion, known as congestive hepatopathy (CH), occurs as a result of hepatic outflow obstruction, a condition most commonly observed in congestive heart failure. Chronic hepatic congestion can eventually result in hepatic fibrosis. Liver specimens of patients with hepatic congestion are histologically characterized by sinusoidal engorgement and hemorrhagic necrosis in the perivenular areas of the hepatic acini, which leads to sinusoidal fibrosis and ultimately to bridging fibrosis between adjacent central veins.^{1,2} Our understanding of fibrogenesis in CH has largely come from pathological examinations of human samples. The mechanisms have remained unclear partly as a result of the lack of appropriate experimental models.

In the current issue of HEPATOLOGY, Simonetto et al.³ developed a murine model of CH through partial ligation of the inferior vena cava (pIVCL). Using this model and an *in vitro* cell culture system, they demonstrated that chronic hepatic congestion causes sinusoidal thrombus formation as well as sinusoidal stretch, which both facilitate fibronectin (FN) fibril assembly by hepatic stellate cells (HSCs), an early step in extracellular matrix (ECM) deposition, and, eventually, hepatic fibrosis.³ This work is novel and important, particularly because of the development of a relatively easy surgical procedure to generate hepatic

congestion in rodents, which allowed them to investigate a mechanistic link between CH and fibrosis.

In their pIVCL model, the inferior vena cava (IVC) was ligated along with a sterile steel wire of 0.6 mm in diameter. The wire was placed alongside the IVC and the two ligated together, with the wire acting as a spacer or placeholder for the ligature. The wire was removed immediately after the ligation, which reduced the IVC diameter by approximately 70%. The investigators characterized this model intensively and verified that mice given pIVCL presented pathological features similar to those observed in patients with CH, including the development of fibrosis. An exception was cardiac output. Though reduced cardiac output was reported in patients, no reductions were observed in this mouse model.

There were two key observations in their pIVCL model. One was minimal inflammatory activity in the liver, despite the development of fibrosis. Given that chronic inflammation has a pivotal role in the majority of fibrotic cases, this was a unique feature and suggested a noninflammatory mechanism of fibrogenesis. In fact, minimal hepatic inflammation was observed in patients with the Fontan circulation, another cause of cardiac disease-related hepatic congestion, suggesting that fibrosis can develop independently of inflammation in this condition.⁴ The other was sinusoidal thrombus formation, which was evident by the presence of fibrin in liver specimens of pIVCL mice as well as those of patients with CH. The investigators examined whether disruption of the coagulation process by pharmacological (warfarin treatment) and genetic (tissue factor pathway inhibitor [TFPI]-overexpressing mice) measures reduces fibrosis in the pIVCL model (Fig. 1). TFPI is an endogenous inhibitor of the extrinsic coagulation pathway,⁵ and thus mice overexpressing TFPI prevent thrombosis. These two approaches significantly reduced intrahepatic fibrin levels and fibrosis, indicating an effect of thrombosis on fibrogenesis in CH.

How does thrombus formation contribute to fibrosis? The coagulation process generates mature fibrin clots through cleavage of circulating fibrinogen by the action of thrombin, a potent plasma protease.⁶ Fibrin facilitates binding of FN to fibril (FN fibril

Abbreviations: CH, congestive hepatopathy; ECs, endothelial cells; ECM, extracellular matrix; FN, fibronectin; HSCs, hepatic stellate cells; IVC, inferior vena cava; LMWH, low-molecular-weight heparin; LSECs, liver sinusoidal endothelial cells; NO, nitric oxide; pIVCL, partial ligation of the inferior vena cava; TFPI, tissue factor pathway inhibitor.

Y.I. is supported by R01 DK082600 from the National Institutes of Health/ National Institute of Diabetes and Digestive and Kidney Diseases.

Received September 12, 2014; accepted September 30, 2014.

Address reprint requests to: Yasuko Iwakiri, Ph.D., Department of Internal Medicine, Section of Digestive Diseases, Yale University School of Medicine, 333 Cedar Street, New Haven, CT 06520-8000. E-mail: yasuko.iwakiri@yale.edu; fax: +1-203-785-7273.

Copyright © 2014 by the American Association for the Study of Liver Diseases.

View this article online at wileyonlinelibrary.com.

DOI 10.1002/hep.27550

Potential conflict of interest: Nothing to report.

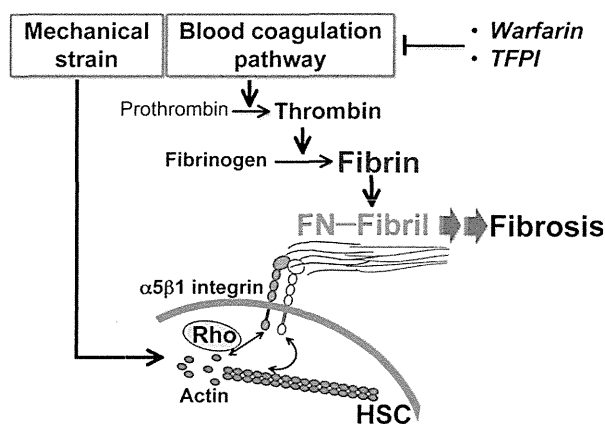


Fig. 1. Sinusoidal thrombosis and mechanical strain lead to liver fibrosis in CH. In the coagulation process, mature fibrin clots are formed through cleavage of circulating fibrinogen by the action of thrombin, a potent plasma protease. Fibrin formation promotes binding of FN to fibril (FN fibril assembly), a key process of the development of a provisional ECM. FN fibril assembly is initiated by binding of FN to integrins, mainly $\alpha 5\beta 1$ integrin, which is assembled with intracellular contractile filamentous actin in HSCs. The assembly of filamentous actin is regulated by bidirectional signaling between Rho kinase activity and integrins. Similarly, mechanical strain resulting from hepatic congestion promotes FN fibril assembly in an integrin- and actin-dependent manner.

assembly),⁷ a key process for the development of a provisional ECM. FN fibril assembly is initiated by binding of FN to integrins, mainly $\alpha 5\beta 1$ integrin, followed by cytoskeletal rearrangements and Rho-dependent cellular contractions.⁸ The investigators verified that fibrin stimulates FN fibril assembly by HSCs in an integrin- and actin-dependent manner, linking hepatic thrombosis to fibrosis. In addition, they demonstrated that mechanical forces, such as sinusoidal stretch, could also promote FN fibril assembly (Fig. 1). Hepatic congestion could increase intrahepatic pressure (stress), resulting in a stretch of endothelial cells (ECs) and HSCs. The effects of mechanical strain on ECs and HSCs have not been well characterized.

In this study, a series of *in vivo* and *in vitro* experiments were logically designed and thoroughly executed, which led to the demonstration of two new potential mechanisms of fibrogenesis, namely, thrombus- and mechanical force-mediated fibrogenesis. However, given that every novel study raises questions, so does this one. Several come to mind. What would happen in pIVCL mice, when the postoperation period is extended longer than the current 6 weeks? Given a relatively mild degree of fibrosis at 6 weeks of pIVCL, do mice with pIVCL develop fibrosis further, if they are kept longer? At that time point, would inflammation still not be observed? Would there be

development of edema or ascites, which is also a feature of advanced CH?¹

Given the development of fibrosis in the pericentral and sinusoidal areas in CH, it may also be interesting to examine the involvement of fibroblasts around the central vein in fibrogenesis. Hemodynamic changes resulting from hepatic congestion may change local mechanical forces, which could facilitate activation of pericentral fibroblasts, as well as HSCs, to profibrotic myofibroblasts⁹ and thereby contribute to ECM deposition. Furthermore, given that liver sinusoidal endothelial cells (LSECs) are exposed to hemodynamic changes directly,¹⁰ they may also have a role in this process. In general, the effects of hemodynamic changes and related local mechanical changes on fibrogenesis are not well understood. The pIVCL model will be a good tool for studies in this area.

There may also be an involvement of nitric oxide (NO) in CH. Sinusoidal stretch resulting from hepatic congestion may disturb LSEC function. A major feature of EC dysfunction is diminished NO production.¹¹ EC-derived NO inhibits platelet aggregation, thereby inhibiting thrombosis.¹² Diminished NO may contribute to increased thrombus formation in CH. Given the vascular aspects of congenic hepatopathy, the role of NO in this disease would be an area warranting additional investigation.

This study again raises important questions of whether or not anticoagulant therapy has a role in patients with liver fibrosis/cirrhosis as well as in those patients with hepatic congestion. The clotting aspect of fibrosis/cirrhosis has been suggested. Besides the present study, one study reported on the efficacy of warfarin in prevention of hepatic fibrogenesis in mice exposed to carbon tetrachloride (CCl₄).¹³ Another study reported that a low-molecular-weight heparin (LMWH) reduced fibrogenesis in rats with CCl₄ treatment.¹⁴ Moreover, efficacy of enoxaparin, an LMWH, was shown for hepatic decompensation, as well as the treatment and prevention of portal vein thrombosis, in patients with advanced cirrhosis.¹⁵

All these and other questions may be answered, in part, with studies using this pIVCL model. The pIVCL model will be beneficial for understanding the pathogenesis and -physiology of CH as well as other similar diseases, such as veno-occlusive disease and Budd-Chiari syndrome, and thus for developing therapeutic strategies for these diseases. This model will also be useful for understanding the effects of hemodynamic changes in the hepatic circulation on liver pathophysiology in general, which also has significant implications in the liver-heart axis, a well-recognized, but underexplored, interaction.

Acknowledgment: The authors thank Dr. Chuhan Chung for his careful review of the manuscript and helpful suggestions.

HISASHI HIDAKA, M.D., PH.D.¹
 AND YASUKO IWAKIRI, PH.D.²
¹*Department of Gastroenterology
 Internal Medicine
 Kitasato University School of Medicine
 Sagamihara, Japan*
²*Department of Internal Medicine
 Section of Digestive Diseases
 Yale University School of Medicine
 New Haven, CT*

References

- Giallourakis CC, Rosenberg PM, Friedman LS. The liver in heart failure. *Clin Liver Dis* 2002;6:947-967.
- Bayraktar UD, Seren S, Bayraktar Y. Hepatic venous outflow obstruction: three similar syndromes. *World J Gastroenterol* 2007;13:1912-1927.
- Simonetto DA, Yang HY, Yin M, deAssuncao TM, Kwon JH, Hilsher M, et al. Chronic passive venous congestion drives hepatic fibrogenesis via sinusoidal thrombosis and mechanical forces. *HEPATOLOGY* 2014;61:648-659.
- Kendall TJ, Stedman B, Hacking N, Haw M, Vettukattill JJ, Salmon AP, et al. Hepatic fibrosis and cirrhosis in the Fontan circulation: a detailed morphological study. *J Clin Pathol* 2008;61:504-508.
- Lwaleed BA, Bass PS. Tissue factor pathway inhibitor: structure, biology and involvement in disease. *J Pathol* 2006;208:327-339.
- Wolberg AS. Thrombin generation and fibrin clot structure. *Blood Rev* 2007;21:131-142.
- Greiling D, Clark RA. Fibronectin provides a conduit for fibroblast transmigration from collagenous stroma into fibrin clot provisional matrix. *J Cell Sci* 1997;110:861-870.
- Wierzbicka-Patynowski I, Schwarzbauer JE. The ins and outs of fibronectin matrix assembly. *J Cell Sci* 2003;116:3269-3276.
- Tomasek JJ, Gabbiani G, Hinz B, Chaponnier C, Brown RA. Myofibroblasts and mechano-regulation of connective tissue remodelling. *Nat Rev Mol Cell Biol* 2002;3:349-363.
- Iwakiri Y, Shah V, Rockey DC. Vascular pathobiology in chronic liver disease and cirrhosis—current status and future directions. *J Hepatol* 2014;61:912-924.
- Iwakiri Y. Endothelial dysfunction in the regulation of cirrhosis and portal hypertension. *Liver Int* 2012;32:199-213.
- Kader KN, Akella R, Ziats NP, Lakey LA, Harasaki H, Ranieri JP, et al. eNOS-overexpressing endothelial cells inhibit platelet aggregation and smooth muscle cell proliferation in vitro. *Tissue Eng* 2000;6:241-251.
- Anstee QM, Goldin RD, Wright M, Martinelli A, Cox R, Thursz MR. Coagulation status modulates murine hepatic fibrogenesis: implications for the development of novel therapies. *J Thromb Haemost* 2008;6:1336-1343.
- Abe W, Ikejima K, Lang T, Okumura K, Enomoto N, Kitamura T, et al. Low molecular weight heparin prevents hepatic fibrogenesis caused by carbon tetrachloride in the rat. *J Hepatol* 2007;46:286-294.
- Villa E, Camma C, Marietta M, Luongo M, Critelli R, Colopi S, et al. Enoxaparin prevents portal vein thrombosis and liver decompensation in patients with advanced cirrhosis. *Gastroenterology* 2012;143:1253-1260.

Author names in bold designate shared co-first authorship.

Surgical Technique

Hepaticoduodenostomy in Hepatectomy for Perihilarcholangiocarcinoma: A Preliminary Report

Hiroshi Yoshida^{1*}, Yasuhiro Mamada², Nobuhiko Taniai², Hiroshi Makino¹, Tadashi Yokoyama¹, Hiroshi Maruyama¹, Atsushi Hirakata¹, Masahiro Hotta¹ and Eiji Uchida²

¹Department of Surgery, Nippon Medical School Tama Nagayama Hospital, Japan

²Department of Surgery, Nippon Medical School, Japan

*Corresponding author: Hiroshi Yoshida, Department of Surgery, Nippon Medical School Tama Nagayama Hospital, 1-7-1, Nagayama, Tama-city, Tokyo, 206-8512, Japan, Tel: 81423712111; Fax: 81423727384; Email: hiroshiy@nms.ac.jp

Received: February 08, 2014; Accepted: April 18, 2014; Published: April 21, 2014

Abstract

A Roux-en-Y anastomosis fashioned from the jejunum (i.e., hepaticojejunostomy) is usually used to reconstruct the biliary system in hepatectomy. In this study, we review our experience with hepaticoduodenostomy (HD) as an alternative to Roux-en-Y biliary anastomosis in patients undergoing hepatectomy for perihilarcholangiocarcinoma, report our preliminary findings in 2 patients, and speculate on future applications. Laparotomy was performed using a Kent retractor. Wide Kocherization of the duodenum was done to provide a tension-free anastomosis to the hepatic duct. The Kent retractor was released transiently, and the anastomosis was confirmed to be free of tension. Hepatectomy and excision of the common bile duct were performed. In patients with short distances between the hepatic ducts, a hepaticoplasty was performed. A 10-Fr silicon drain with channels along the sides, approximately 20 mm in length, was used as an internal stent. HD was performed with a single-layer anastomosis with continuous sutures. No complication occurred after HD. Our initial experience suggests that HD may be a viable alternative to Roux-en-Y biliary anastomosis in patients undergoing hepatectomy for perihilarcholangiocarcinoma.

Keywords: Hepaticoduodenostomy; Hepatectomy; Perihilarcholangiocarcinoma

Introduction

A Roux-en-Y anastomosis fashioned from the jejunum (i.e., hepaticojejunostomy [HJ]) is usually used to reconstruct the biliary system in patients undergoing hepatectomy for perihilarcholangiocarcinoma [1]. Recently, reconstruction by hepaticoduodenostomy (HD) or choledochoduodenostomy has been recommended instead of reconstruction by HJ or choledochojejunostomy [2-14]. Complications such as biliary leakage and cholangitis are well documented after HJ and choledochojejunostomy [15-19]. Moreover, the biliary tree is difficult to access endoscopically in patients undergoing enteric reconstruction using a Roux-en-Y anastomosis to the jejunum [20]. HD offers the possible advantage of simple postoperative access to the biliary system by endoscopy and avoids the complications associated with HJ [2].

In this study, we review our experience with HD as an alternative to Roux-en-Y biliary anastomosis in patients undergoing hepatectomy for perihilarcholangiocarcinoma, report our preliminary findings in 2 patients, and speculate on future applications.

Case 1

A 74-year-old woman was admitted because of a dilated left intrahepatic bile duct. Previously, she had undergone a right colectomy because of colonic carcinoma. However, minor leakage of the anastomosis occurred, and reoperation (drainage) was performed. After that, ileus developed and reoperation was done again. Computed tomography revealed dilatation of the left intrahepatic bile duct and mild dilatation of the right posterior intrahepatic duct

(Figure 1). Drip infusion cholangiography revealed only the right anterior intrahepatic duct and stenosis at the hepatic hilum (Figure 2). Perihilarcholangiocarcinoma was diagnosed.

Surgical procedures

Laparotomy was performed using a Kent retractor. Severe adhesions of the jejunum were detected, precluding the use of a Roux-en-Y anastomosis fashioned from the jejunum. After Kocherization of the duodenum to provide a tension-free anastomosis to the hepatic

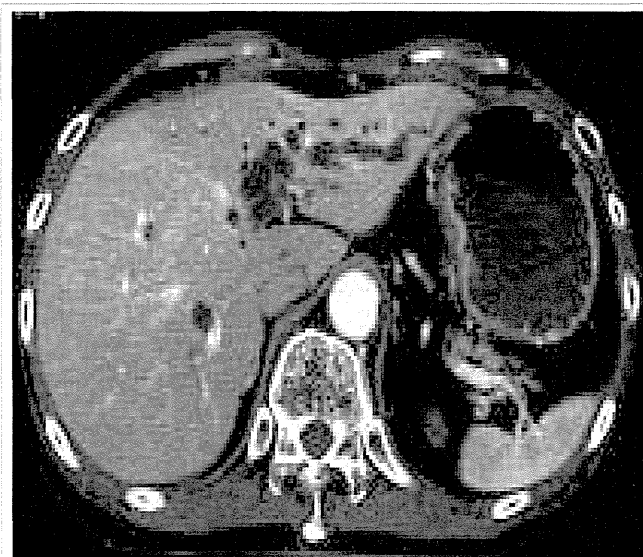


Figure 1: Computed tomography revealed dilatation of the left intrahepatic bile duct and mild dilatation of the right posterior intrahepatic duct.



Figure 2: Drip infusion cholangiography revealed only the right anterior intrahepatic duct and stenosis at the hepatic hilum.

duct, an extended left hepatectomy with excision of the common bile duct and lymph-node dissection was performed. Intraoperative pathological examinations revealed that the stumps of the right intrahepatic bile ducts were negative for carcinoma. There were triple lumens of the right anterior bile ducts and double lumens of the right posterior bile ducts. Hepaticoplasty (i.e., the adjacent walls of the hepatic ducts were sutured together with single stitches using 6-0 polydioxane [PDS, Ethicon, NJ, USA] to obtain a single lumen for biliary anastomosis) was performed to make double lumens of the right anterior bile ducts and a single lumen of the right posterior bile duct. Unexpectedly, the duodenum was distant from the hepatic ducts. To provide a tension-free anastomosis, wide Kocherization of the duodenum was performed again, and the right gastroepiploic artery and vein were cut. The Kent retractor was released transiently, and the anastomosis was confirmed to be tension-free. As an internal stent, a 10-Fr silicon drain with channels along the sides (BLAKE Silicone Drain, Ethicon, NJ, USA), approximately 20 mm in length, was used [21]. Before completing suture of the posterior row, the

stent was inserted into each lumen. Five stents were placed within the hepatic duct and duodenal lumen to serve as the internal stents for the anastomosis. The stent was fixed to the anterior row of stitches with 5-0 polydioxane sutures. Three anastomoses of the intrahepatic bile ducts to the duodenum were established by means of a single-layer anastomosis with continuous sutures (5-0 polydioxane) (Figure 3). Fixation of the greater omentum to the peritoneum was not necessary to prevent delayed gastric emptying [22,23] because the stomach could not come in contact with the cut surface of the liver, a potential cause of adhesion.

The postoperative course was uneventful, and the patient was discharged on postoperative day 12. After discharge, upper gastrointestinal endoscopy revealed no duodeno gastric bile reflux.

Case 2

A 76-year-old man with dilatation of the left intrahepatic duct was admitted. Previously, he had undergone a distal gastrectomy (Billroth II reconstruction) because of gastric carcinoma. Computed tomography and magnetic resonance cholangiopancreatography revealed the dilated left intrahepatic bile duct (Figure 4,5). Perihilar cholangiocarcinoma was diagnosed.

Surgical procedures

Laparotomy was performed using a Kent retractor. Adhesions of the jejunum were detected. Wide Kocherization of the duodenal stump was performed to provide a tension-free anastomosis. The Kent retractor was released transiently, and the anastomosis was confirmed to be free of tension. An extended left hepatectomy with excision of the common bile duct and lymph-node dissection was performed. Intraoperative pathological examinations revealed that the stump of the right hepatic duct was negative for carcinoma. Because the right hepatic duct had a single lumen, hepaticoplasty was unnecessary. HD was performed using a single-layer anastomosis with continuous sutures (5-0 polydioxane). After completing suture of the posterior row, the stent was inserted into the hepatic duct. As internal stents, 10-Fr silicon drains with channels along the sides, approximately 20 mm in length, were used. The stent was fixed to the anterior row of stitches with 5-0 polydioxane sutures. Anastomosis of the right hepatic duct to the duodenal stump was established

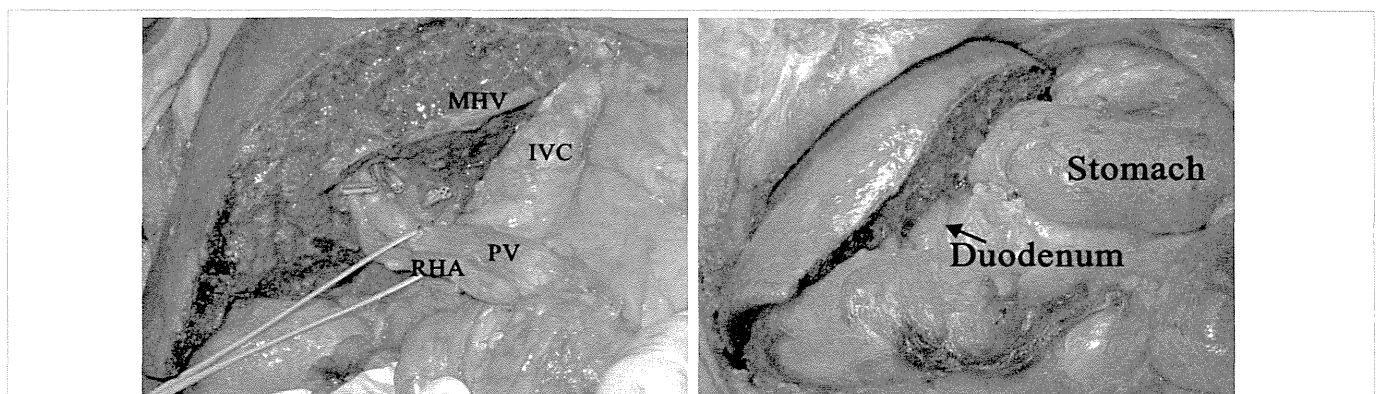


Figure 3: Before completing suture of the posterior row, the stent was inserted into each lumen. Five stents were placed within the hepatic duct and duodenal lumen to serve as the internal stents for the anastomosis. The stent was fixed to the anterior row of stitches with 5-0 polydioxane sutures. MHV: middle hepatic vein, IVC: inferior vena cava, PV: portal vein, RHA: right hepatic artery (a). Three anastomoses of the intrahepatic bile ducts to the duodenum were established by means of a single-layer anastomosis with continuous sutures (b).